Safety Evaluation on LNG Bunkering:

To Enhance Practical Establishment of Safety Zone

Byongug Jeong [a],*, Sayyoon Park[b], Seungman Ha[c], Jae-ung Lee[d]

[a] *Department of Naval Architecture, Ocean and Marine Engineering, University of Strathclyde, 100 Montrose Street, Glasgow, G4 0LZ, UK*

[b] *Daewoo Ship Building & Marine Engineering (DSME), Geo-je 53302, Korea*

[c]*Korean Resister of Shipping, 36 Myeongji Ocean City 9-ro, Gangseo-gu, Busan, Korea*

[d]*Department of Marine System Engineering, Korea Maritime and Ocean University, Taejong-ro 727, Yeongdo-Gu, Busan, 49112, Republic of Korea*

**corresponding author* e-mail: Byongug.jeong@strath.ac.uk, phone: +44(0)7425694809

Abstract

This paper is to evaluate the LNG bunkering safety for a 50,000 dead weight tonnage bulk carrier renowned as the world first LNG fuelled bulk carrier. To establish a proper level of the safety zone against the potential risk of gas release from the LNG bunkering systems encompassing from truck to ship, it introduces an enhanced quantitative risk assessment process with two key ideas: firstly, the integration of the population-independent analysis with the population-dependent analysis, and secondly, the combination between the probabilistic analysis and CFD simulation for gas dispersion. Research results reveal that the appropriate levels of the safe zone can be set at 28.8 m in 1E-4 /year criterion that concerns the individual risk of a fatality at the given distance to the risk source of 1 in 10,000 years, whereas at 46.6 m (in 1E-5 /year criterion) and at 213.3 m (in 1E-6 / year criterion) when the area within 5 % and higher gas concentration in air is regarded the critical zone. On the other hand, in case of the critical area considered to be within 2.5 % and higher gas concentration in air, the safety zone will much expand to 34.9 m (in 1E-4 /year criterion), 80.4 m (in 1E-5 /year criterion) and 541.8 m (in 1E-6 /year criterion). These dissimilarities suggest that LNG bunkering ports pay attention to selecting appropriate safety criteria which would considerably change the range of safety zones. The case study also demonstrates the effectiveness of the proposed approach that can remedy the shortcomings/shortfalls of existing technical and regulatory guidance on establishing the zones. It is, therefore, believed that the risk assessment approach proposed in this paper can contribute to

determining the appropriate level of safety zones whereas providing practical insight into port authorities and flag states.

Keywords; LNG bunkering, LNG-fuelled ship, safety zone, flash fire, gas dispersion, LNG fire/explosion

1 Introduction

1.1 Background

International Maritime Organization (IMO) has recently adopted a new Resolution MEPC.304 (72) with a series of ambitious strategies on curbing greenhouse gas emissions (GHGs) from ship activities (IMO, 2018). Along with this, several stringent regulations to limit nitrogen oxides (NO_x), Sulphur oxides (SO_x) and particulate matter (PM) from ship exhaust gases have been introduced at both international and local levels. Such zealous legislation works urge us to trust that cleaner production and greener sea affair are one of the most urgent issues in the marine industry. Following this trend, the use of liquefied natural gas (LNG) as an alternative marine fuel has increasingly attracted the attention of maritime stakeholders.

The history of LNG-fueled ships started last century while on 20th March 2017 the number of LNG-fueled vessels, other than LNG carriers, has marked at 103 units in service and 97 units on order; a 23 % annual increase on average (Corkhill, 2018). To support their operation, LNG bunkering facilities have been aspiringly planned and constructed in major regions of Europe, USA and Asia. In particular, Europe has a remarkable achievement in bountiful LNG bunkering facilities covering from the Baltic Sea to the North Sea and the Mediterranean Sea (GIE, 2018).

On the other hand, LNG is cryogenic liquid obtained by condensing natural gas to its boiling temperature of roughly -162 °C and so reducing its volume 600 times. That way facilitates transport and storage strongly. Due to the very low boiling temperature, this substance, however, is normally stored and handled through cryogenically-insulated compartment systems. An accidental LNG leak from any part of these systems may lead to rapid phase transition as well as drastic expansion in volume, forming an excessive flammable cloud with air mixture. Such an uncontrollable release may expose the ship and crews to various risks, such as asphyxiation, cryogenic burns, structural embrittlement and fire and explosion (ISO, 2015a). A number of research warns the potential accidents associated with LNG release (Choi et al., 2018; Dan et al., 2014; Dasgotra et al., 2018; Jeong et al., 2017b; Luo et al., 2018; Park et al., 2017; Park et al., 2018; Vílchez et al., 2013). Tan et al. (2014) interestingly carried out a qualitative risk assessment pertinent to LNG release in Beijing city during the Olympic Games, presenting the significant impact of accidents on populated areas.

Likewise, LNG bunkering implies potential risks directly related to the activity of liquid transfer and vapour return. A number of LNG-related accidents have been reported across industries over the decades (Hamutuk, 2008; ISO, 2013b, 2015a; Woodward and Pitbaldo, 2010). For LNG bunkering alone, the Norwegian Maritime Authority reported four LNG spill accidents - one of them resulted in a cryogenic burn on a crew’s hand and legs (K, 2015). Germany and Norway (2012) identified potential hazards associated with using LNG as a marine fuel and their findings were submitted to IMO as an information document.

To respond to the potential risks of using LNG as a marine fuel, various codes, rules, standards and guidance have been introduced both internationally and locally over the decade (ABS, 2012; BV, 2012; DNV, 2011; Gopalaswami et al., 2017; Lee et al., 2015; Register, 2011). On the other hand, ABS (2014) summarized current LNG bunker regulations and guidelines, emphasizing that there was no direct regulation of LNG bunkering.

Regarding a series of ISO standards, ISO 16903 (ISO, 2013a) pointed out the dangers of maritime LNG transportation, providing a certain level of safety guidelines. The concept of the safety zone for LNG bunkering was proposed by ISO / TS 18683 (ISO, 2015a) that recommends installing a safety zone encompassing the supply point on the terminal side and the bunkering station on the ship to limit all non-essential personnel during bunkering, thereby minimising the possibility of ignition and human injury. However, judging that the past standards were inadequate, ISO developed new standards of ISO / TS 16901 (ISO, 2015b) which suggests the implementation of risk assessment for establishing the safety zone.

Nevertheless, these standards do not clearly provide specific guidelines on the procedure of risk assessment other than stating that either deterministic or probabilistic approach can be acceptable. More sophistically, Jeong et al. (Jeong et al., 2017a; Jeong et al., 2017b) have addressed the shortcomings of current regulations and practices, pointing out various regulatory ambiguities and the lack of quantified safety requirements, particularly when establishing the safety zone for LNG bunkering.

1.2 Remarkable past research

While several safety research on LNG-fueled ships both qualitatively and quantitatively have been conducted over the last decade, Jeong et al. (2018) discussed novelties and limitations of their findings. This paper, on the other hand, is to emphasize recent notable publications directly related to this study.

> While many flag states and ports were struggling to confirm the proper level of the safety zone during LNG bunkering, the Port of Gothenburg managed to establish the zones using the quantitative risk assessment in collaboration with DNVGL (2014). They estimated the risk levels associated with the LNG bunkering in several scenarios and determined the safety distances ranged from 15 m up to 25 m which were placed within the acceptable level of an undesirable event to be once a thousand year (10^{-3} / year). This study was noteworthy as the first systematic investigation of LNG bunkering safety. To analyze the fire/explosion impacts, it adopted analytical and

empirical models that would be a simple approach but less reliable when compared to the computer-aided simulations. Similar research scope and limitations can be found in Jeong et al. (Jeong et al., 2017a; Jeong et al., 2017b). Pitblado et al. (2006) applied DNV risk assessment software to determine the LNG hazardous zones in LNG terminals. The accidental scenarios were established based on worst-case scenarios and the research suggested large-scale experiments or systematic safety investigation to be carried out for reducing uncertainties.

Methodologically, Jeong et al. (2018) introduced a practical approach to addressing the pitfalls of the current guidelines and research approaches pertinent to establishing the safety zone for LNG bunkering; the proposed approach was expressed by the implementation of population-independent and population-dependent analyses in series, thereby improving the reliability as well as practicability of results. This previous study focused on the general investigation of key parameters affecting the level of the safety zone in a site-independent manner. However, given the fact that the effects of fire and explosion are greatly influenced by geometry or meteorology conditions, the past research has suggested a further work to be done in order to confirm the effectiveness of the proposed approach in a site-specific manner.

Using a consequence-based KPI (Key performance indicator) approach as a quantifiable measure to assess the feasibility of LNG bunkering, Iannaccone et al. (2019) carried out the safety assessment of LNG bunkering process which were compared to the conventional diesel bunkering. Research results indicated that the complexity in the LNG transfer operation, equipment as well as the high flammability were regarded as key points in diminishing the safety of LNG bunkering.

There are also some remarkable research on investigating the behavior of LNG dispersion using CFD simulations. The research of Sun et al. (2017) was the first attempt to use 3D simulations to investigate the consequences of unwanted LNG release during the bunkering. They characterized LNG release by different risk types, vapor dispersion and radiation resistance in both qualitative and quantitative views. Park et al. (2018) was focused on identifying the parametric influences on the gas dispersion in aids of 3D simulations under the ship-to-ship LNG bunkering environment.

In addition, similar research on investigating the impact of LNG dispersion can be found in other industrial sectors. With Gexcon AS FLACS (Flame acceleration simulator) Code, Dasgotra et al. (2018) investigated the impact of gas release from oil and gas refineries/storage terminals. Flow rates, ambient conditions, and duration of release were found to be key variables to estimate the dispersion ranges. It indicated the 3D simulations with detailed modeling would help better understanding of the dispersion behavior, compared to the older phenomenological model. Hansen et al. (2010) introduced an interesting study on validation FLACS using experimental data sets (33 field-scale and wind tunnel tests) for natural gas dispersion. Since most experimental cases were consistent with simulation results, the research has suggested the FLACS can be a suitable model for accurately simulating the dispersion of vapor.

Numerical simulation of LNG release and dispersion using a multiphase CFD model were also carried out by several researchers (Giannissi et al., 2013; Luo et al., 2018). Intriguingly, Vílchez et al. (2013) investigated the relationship between the LFL (lower flammable level) distance and visible contour of LNG gas cloud. As a result, they haves introduced a safety factor that is expressed by the ratio between the LFL distance and those visible contours that generally depends on the moisture content of the atmosphere. It could be regarded as an indicator that helps to identify the danger of cloud ignition and flash fire. In aids of the CFD models, Choi et al. (2018) investigated the impacts of initial conditions of LNG gas dispersion particularly with initial temperature and the obstacles surrounding an LNG bunkering terminal. It particularly discussed the significance of the impact of the cylindrical obstacles and the range of initial temperature - 50 to - 150 ºC. A similar study can be found in several research by Gavelli et al. (2010) and Parihar et al. (2011) where the LNG spill, evaporation and dispersion were calculated in a combination of analytical calculation and CFD simulations. Those studies underscore that importance of setting up the accurate initial conditions for CFD simulation.

In addition to computational simulations, there can be found a few experimental research on LNG release associated with LNG transport and storage process. Wang et al. (2019) carried out an experimental study to estimate the LNG gas-induced fire impacts. Gopalaswami et al. (2017) conducted an experimental and numerical study (CFD based) of LNG gas dispersion from the LNG pool on water. It was found that the influence of wind was shown to affect the formation of vapour cloud as providing additional heat and unsaturation.

Previous studies have unanimously suggested that CFD or experiment-based studies provide more accurate and realistic results on the prediction of the behavior of LNG gas dispersion than analytical models. The scope of those research was, however, due largely limited to investigating the severity of LNG leaks in a deterministic approach while disregarding the probability of its occurrence. Consequently, those works were not able to offer a clear insight into the LNG bunkering risk that should be expressed as the combination of the probability of LNG incidents with their severity.

Villa et al. (2016) published a review paper on investigating the risk assessment progress applied to the chemical industry over the decades. It also provides an overview on the shortcomings of conventional quantitative risk assessment, which has not been improved since the early 1980s. Swuste et al. (2018) carried out a similar study that overviewed safety management systems, models for gas incidents across the industries. Given the limitations of past approaches, the review paper suggested a dynamic risk assessment to apply realistic data for case studies. This paper is in consistent with this suggestion as it presents a better direction for a practical performance of quantitative risk assessment.

1.3 Research aim

Given the methodological limitations of previous research, this paper is to introduce an enhanced approach to establishing safe zones for LNG bunkering. The proposed approach will be used to evaluate the practical level of safety zones for case-specific bunkering conducted by truck to ship (TTS) method. The risk results obtained from population-independent analysis (PIDA) is intended to be compared to those from the population-dependent analysis (PDA) as a verification process which can improve the trustworthiness of the research outputs.

2 Research procedure

The approaches adopted in this paper is an enhanced version of the quantitative risk assessment process preliminarily introduced by Jeong et al. (2018). This approach can be expressed as the combination of the probabilistic analysis and the consequence analysis in aids of the state-of-the-art computer simulation tool, FLACS.

The risk assessment procedure aimed at determining the safety zone for the case ships is overviewed in Fig. 1 which mainly consists of five steps: (1) data collection (2) scenario analysis, (3) frequency analysis, (4) consequence analysis, and (5) risk assessment. This procedure basically follows a probabilistic risk assessment approach guided by IMO (IMO, 2002) but has been revised according to the purpose and the scope of this research.

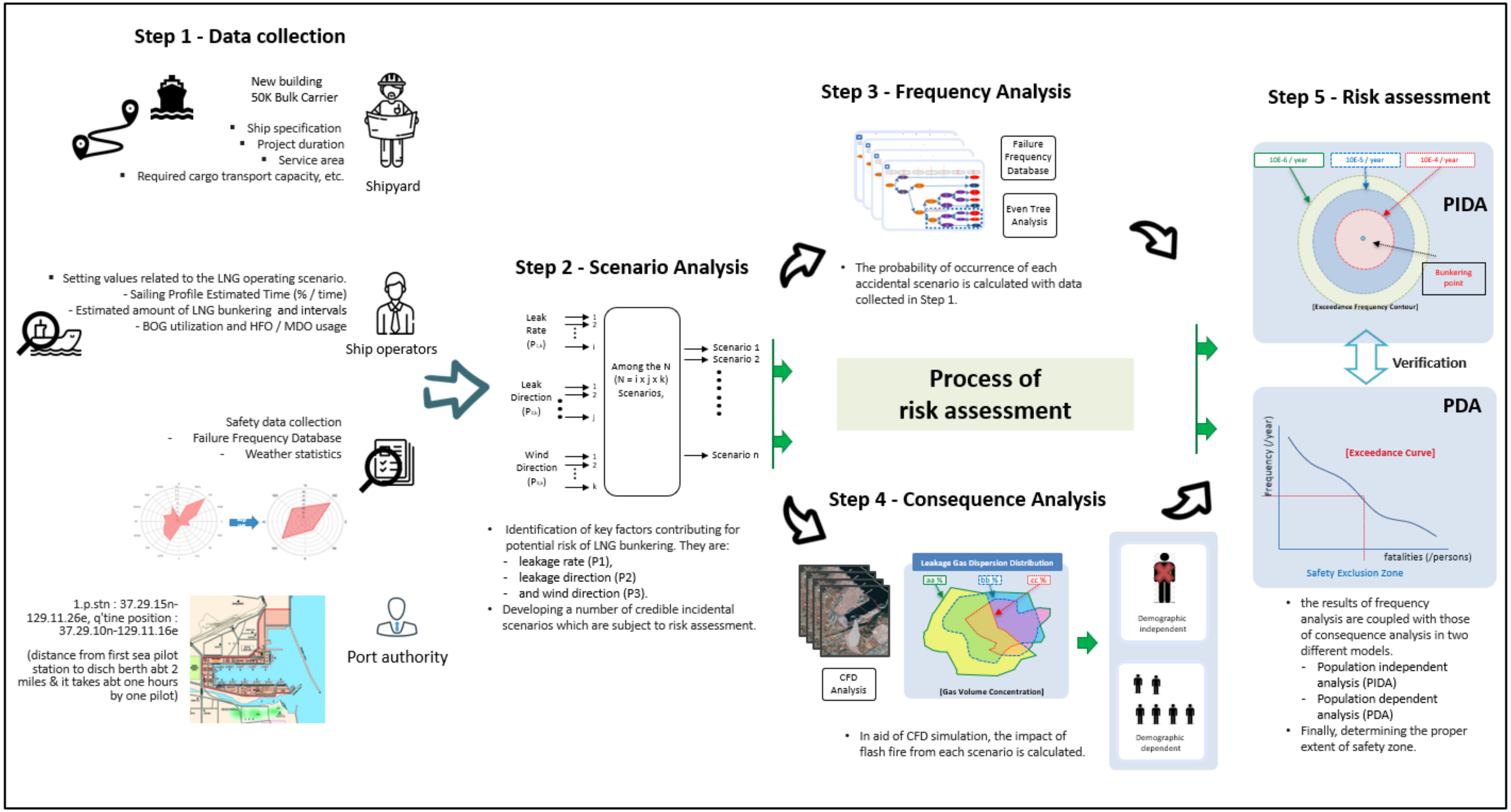

Fig. 1. Outline of the quantitative risk assessment for LNG bunkering.

2.1 Step 1: Data collection

The first step of data collection was designed to carry out the process of gathering and measuring information on the case ship and the port through the field survey. This step can be regarded as a key component of this research to understand the industrial challenges and to capture true-to-life information applicable to the analyses for the next steps from stakeholders.

2.2 Step2: Scenario analysis (hazard identification)

As the second step in Fig. 2, this paper identified various accidental scenarios related to LNG release during bunkering in consideration of the probability of the following parameters: leakage rate (P_1), leakage direction (P_2) and wind direction (P_3). Meanwhile, according to the wind statistics, the wind speed for the research region was largely ranged between 6 and 8 m/s, thereby the average wind speed of 7 m/s was uniformly applied for all the scenarios. All accidental scenarios determined from the scenario analysis were subject to the estimation of the probability of their occurrence and to the evaluation of their consequent impact in the following steps.

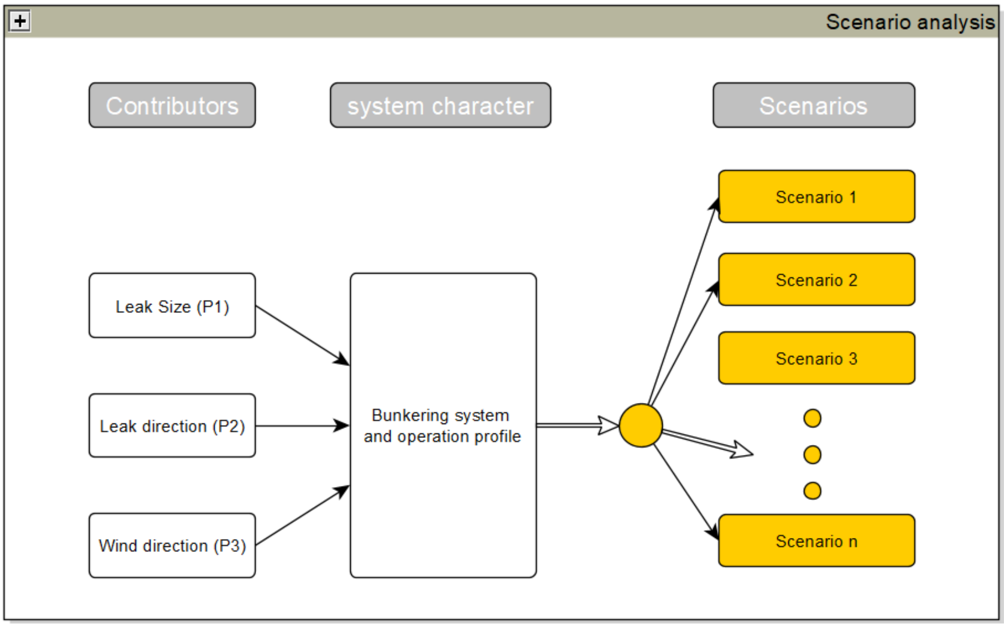

Fig. 2. Outline of scenario analysis.

2.3 Step 3: Frequency analysis

The frequency of each accidental scenario could be calculated by multiplying the probability of each variable at the given condition. P_1 was basically obtained from the DNV failure frequency database (DNV, 2012) for LNG component failures leading to gas/liquid release in various leak hole sizes. The

DNV data was originally collected by the Health and Safety Executive (HES) from operators in the North Sea after the Piper Alpha accident. Although these leaks are not directly related to LNG, but commonly used for LNG risk studies due to the brevity of relevant LNG data.

Given the case model that maximum size of piping system is 150 mm, this study simplified various leak hole sizes into two representative ones by taking a conservative stance; the leakage cases ranging between 1-50mm are represented to 50 mm hole leak ($P_{1,1}$) and those of 50-150 mm are to be 150 mm ($P_{1,2}$).

P_2 is directional due to the position of leak hole (say, Up, Down, Left, Right, Forward, and Backward). Therefore, a 1/6 of the probability was distributed to each leak direction scenario: Up ($P_{2,1}$), Down ($P_{2,2}$), Left ($P_{2,3}$), Right ($P_{2,4}$) and Forward ($P_{2,5}$) and Backward ($P_{2,6}$) respectively. Meanwhile, the variables associated with the wind (P_3) were weighted based on the historical wind statistics (Windfinder, 2018). The original 16 wind directions were integrated into four representative directions: West ($P_{3,1}$), East ($P_{3,2}$), North ($P_{3,3}$), and South ($P_{3,4}$).

Fig. 3 shows the process of the scenario identification and frequency analysis. The results have determined 48 accidental scenarios leading to the flammable gas dispersion whose impacts were investigated through the consequence analysis in the next step.

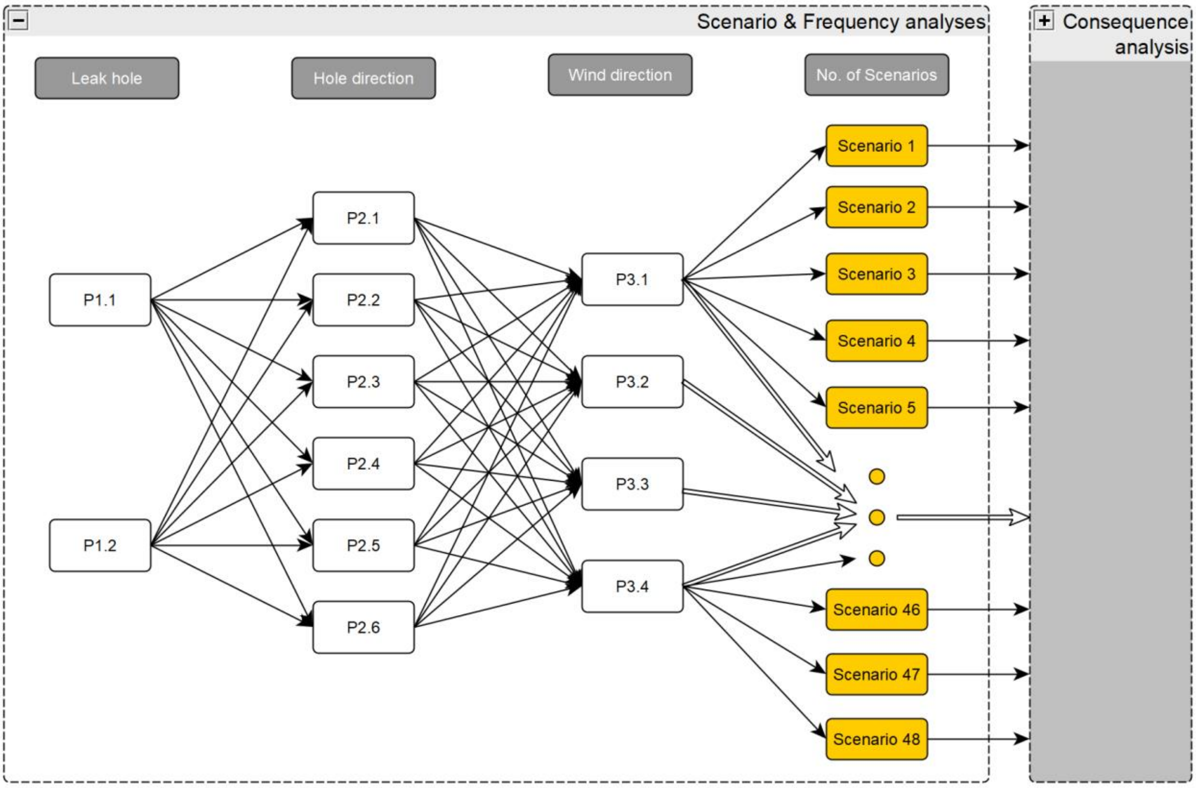

Fig. 3. Outline of scenario identification and frequency analysis.

On the other hand, it should be mentioned that LNG bunkering is a periodical operation rather than a continual operation whereas the DNV data offers the frequencies of leaks based on continual operation. This fact was taken this into account for estimating the frequency of LNG leak during the bunkering by employing the reduction factor representing the ratio of actual operation period per year. As a result, the applied frequencies for LNG leaks will be approximately 2 % of the frequencies pertaining to the continual operation in DNV data.

2.4 Step 4: Consequence analysis

Despite various types of consequences from LNG incidents, this paper is focused on the risk of flash fire which is the most likely to occur as the consequence of LNG leak in open space.

Explosion often refers to a vapor cloud explosion (VCE). It is because high levels of gas congestion in a limited space lead to explosions. In this regard, it is reasonable to assume that this type of incident is more likely to occur in confined spaces rather than open spaces (Dan, 2014). The LNG bunkering for the case ship takes place on the exposed deck that is regarded as an open space both physically and regulatorily. Meanwhile, the analytical calculations conducted by Jeong et al. (2017b) revealed that the impact of jet or pool fire was relatively smaller than that of gas dispersion and flash fire. Given this, the consequence analysis was focused on simulating the gas dispersion that can be converted to flash fire when encountered with an ignition source.

Fig. 4 outlines the consequence analysis. Using the Eq. (1), the analysis was initiated with the calculation of leak rates in representative leak holes and the operating conditions for bunkering. The parameters used in this calculation are based on the data for the case ship.

$$Q = C \times A \times \sqrt{2 \times \rho \times p_g} \qquad \text{Eq. (1)}$$

Where Q is the leak rate [kg/s], C is the discharge coefficient, A is the cross-sectional area of the leak point [m^2], ρ is the density of LNG [kg/m^3], and P_g is the gauge pressure inside the pipe [Pa].
Next, all accidental scenarios, with the estimates of gas leak rates, are investigated to assess the critical boundary of gas dispersion by means of computational fluid dynamics (CFD) method, FLACS Version 10.5. Table 1 presents the general setup information for the simulation.

Table 1. General information on the CFD modelling condition.

Analysis Duration	**Leakage Duration**	**Wind Build-up Time**	**Reference Height of the Wind**	**Ambient Temperature**

110 Seconds	90 Seconds	10 Seconds	10 m	20 ℃
Simulation Volume Sizes [m]	**Boundary Condition [X,Y,Z]**	**Courant-Friedrichs-Levy Number**	**Grid Size [minimum]**	**Grid Size [maximum]**
(2000, 2000, 200)	Wind(Outflow) & Nozzle(Inflow)	CFLC:10 CFLV:1	0.5 m	40 m

ISO standards (ISO 20519:2017) for LNG bunkering requires that ½ LFL should be used for risk assessment and the probability of flammable gas outside the safety zone should be less than 1E-6 per bunkering operation. While providing practical recommendations and guidelines as a principle supervisory frame, ship owners and port authorities are not obligated to fully comply with ISO the standards. The IGF code which the flag states are directly subject to observe not specifically present the safety requirements for the safety zones. Given this, there will be still passibilities on establishing different levels of safety requirements based on the fact that:

Since safety evaluators and flag states may have different views on determining the tolerable level of the gas concentration in air, this paper adopted two different criteria:

- Criterion 1: half-LFL equivalent to 2.5 % of airborne gas concentration by volume;
- Criterion 2: full-LFL equivelent to 5.0 % of airborne gas concentration by volume;

Given this, the critical distances/areas were defined to be the lengths/scopes within those gas concentration levels. Hence, the CFD simulation allows us to observe the dynamic behaviour of gas dispersion at different scenarios, thereby to determine critical zones. The measured critical distance and area were, then, used to indicate the extent of the dangerous area when combined with the frequency analysis results during the next step of risk assessment.

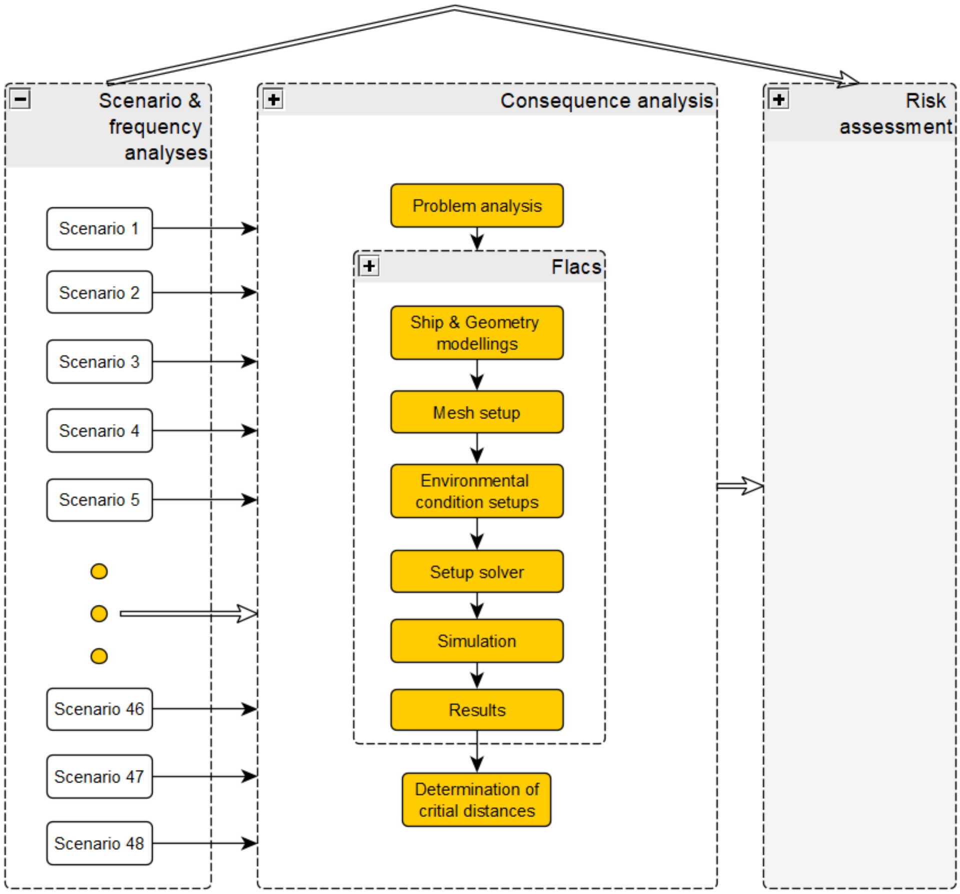

Fig. 4. Outline of consequence analysis.

2.5 Step 5: Risk assessment (Integration)

Fig. 5 shows the process of risk assessment where the results of frequency analysis would be coupled with those of consequence analysis in two different ways: one is with PIDA and the other is with PDA.

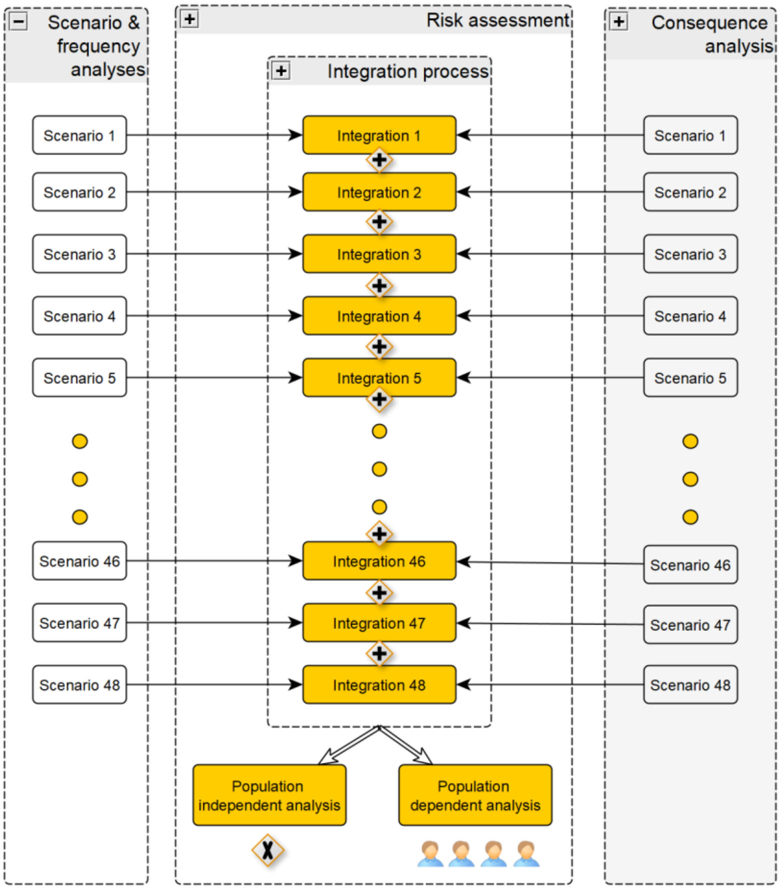

Fig. 5. Outline of risk assessment.

(a) *Population-independent analysis (PIDA)*

The critical distance for each scenario was integrated with the frequency result, and the combined results were expressed in a single analysis plot domain. Therefore, the safety zone was determined as the maximum critical boundary that could reach the marginally tolerable frequency. The results are converted to a form of exceedance frequency contour plot on the bunkering geometry map.

(b) *Population-dependent analysis (PDA)*

In case that the outcome of the consequence is to stand for human fatalities, PIDA has several pitfalls in setting the appropriate level of the safety zone. Given the fact that the higher number of people at danger, the greater the risk, it is important to address the weakness of the PIDA that does not care about the population in place.

To remedy this problem, the PDA, as the post-process of the PIDA, was proposed to convert the consequence results expressed as the critical area of the gas dispersion into the number of casualties within the region. Then, this form of outcomes was combined with the frequency results. The final risk was represented in the F-N curve which could be regarded as a type of risk curve presenting the frequency (F) of causing the number of fatalities per year (N). As a function of N, the graph is plotted on a double logarithmic scale. Results of the PDA were, then, employed to corroborate the pertinence of the safety zone determined through the PIDA.

3 Case Study

The proposed method discussed in the previous section was applied to a case study with a 50,000 DWT bulk carrier of MV 'Green Iris' known to be the world first bulk carrier using LNG as a marine fuel.

3.1 Data collection and Scenario analysis

The case ship specifications are summarized in Table 2. The regular voyage of this ship is limited to a coastal freighter for Korean seas as transporting steel products from Donghae at East Seaport of Gangwon to manufacturing factories in the Gwangyang.

With the 500 m^3 capacity of the LNG fuel tank, the case ship was fitted with a set of MAN B&W main engine (7,250 kW) and two sets of dual fuel generator engines (1,100 kW each). According to shipyard's design guidance, the fuel consumption of the main engine at MCR (maximum continuous rating) was estimated about 17.0 t/day in gas mode whereas 21.3 t/day in oil mode.

When only using the gas mode, the vessel is subject to receiving the LNG bunker every two voyages. Considering one voyage consumes six days on average, each bunkering takes about six hours which account for 2 % of annual service time. Since it was intent to investigate the risk pertinent to LNG bunkering, the scope of analysis was focused on this 2 % of the time duration.

Table 2 Ship description (*by courtesy of ILSHIN Marine Transport Co., Ltd.)*

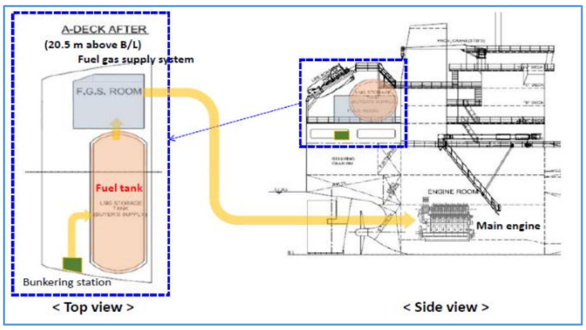

Name	MV ILSHIN GREEN IRIS	Speed recorded (Max. / Average)	14.5 / 13.8 knots
IMO No.	9812602	Service route	KR TGH – KR KAN (265 miles)
Gross Tonnage	31,005 t	Main Engine	B&W 6G50ME-9.5-GI MCR: 7,250 × 88.7 rpm
Deadweight	50,655 t	Fuel consumption	21.3 t/day (oil mode) 17.0 t/day (gas mode)
L × B × D	190.6 × 32.0 × 7.4	G/E	2 sets × 1,100 kW (6L20DF)
LNG fuel supply system			
LNG Fuel tank	IMO Type C, 500m^3 / 7 bar		
LNG supply pump	2 sets of 1,744 kg/h, 182 mTH	High pressure vaporizer	1 set of 1,149 kg/h,-147/45^{o}C
High Pressure pump	2 sets of 1,149 kg/h, 320 bar	Low pressure vaporizer	1 set of 595 kg/h, -163/30^{o}C

What distinguishes it from conventional ship types is that the LNG fuel supply systems - LNG supply pumps, high pressure pumps, low and high pressure vaporizers were fitted in the fuel gas system room adjoining the LNG fuel tank as shown in Table 2.

Fig. 6 shows the arrangement of onboard LNG bunkering system, which mainly consists of pipes, valves, flanges and gauge fittings, with three piping lines: liquid main, vapour return and inert lines. Meanwhile, the truck-to-ship bunkering does not employ the vapour return connection as the reasons that the LNG truck do not have a vapour return facility and the LNG C type tank onboard is designed to keep its pressure lower than the designed pressure without any vapour return. This practice was also confirmed by the curtesy of the case ship operator: ILSHIN Ltd. In addition, the inert gas has no impact of fire/explosion so that the risk assessment was focused on the LNG leak associated with the main line.

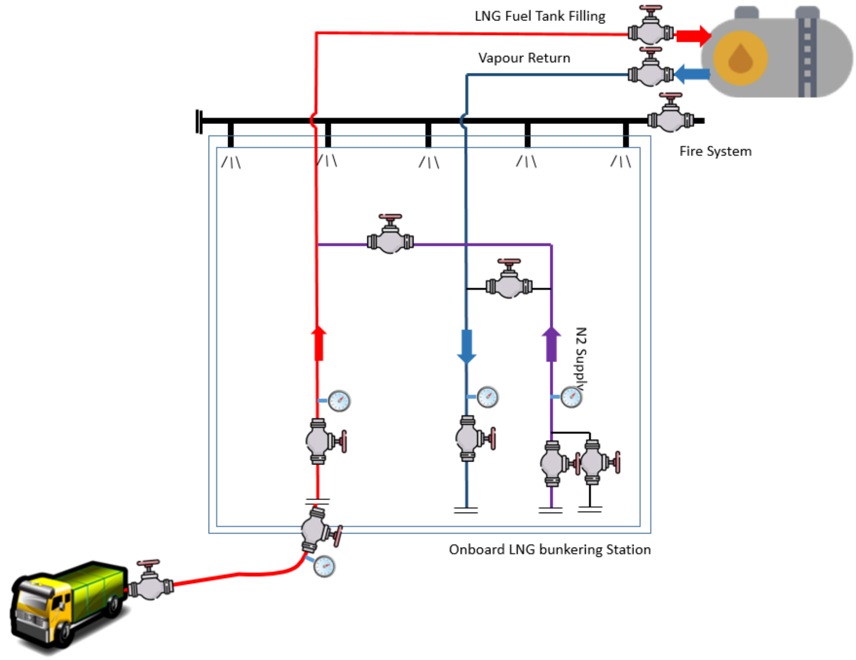

Fig. 6. Arrangement of onboard LNG bunkering system (*by courtesy of ILSHIN Marine Transport Co., Ltd.*).

The supply of LNG bunker is generally carried out with tank lorries whose bunkering system is comprised of similar fittings. The list of equipment for LNG bunkering in both ship and tank lorry sides is presented in Table 3.

Table 3 Equipment for LNG bunkering (*by courtesy of ILSHIN Marine Transport Co., Ltd.*).

Equipment	**Size (mm)**	**Quantity**	
		Receiving side (Case ship)	**Feeder side (Tank lorry)**
ESD Valve	150	1	1
Flange	150	4	4
Manual Valve	150	1	1
Pipe (/m)	150	5	5
Small Gauge Fittings	12.5	5	4
Manual Valve	40	1	1
Flange	40	1	1

3.2 Frequency Analysis

Using DNV failure frequency database (DNV, 2012) described in Section 2, the frequency of each equipment to the failure was calculated based on four (4) representative leak hole sizes: 3mm, 10 mm, 50 mm and 150 mm (full rupture). Then, with a conservative stance, the representative leak hole sizes (3 mm, 10 mm, 50 mm) associated with all equipment were integrated to the 50 mm leak group and 150 mm leak was made another group. Thus, the frequency of 50 mm leak hole group and 150 mm leak hole group and their leak rates were calculated as presented in Table 4. The gauge pressure inside the LNG mainline was set at 3 bar (g) while the density of LNG at the proposed condition was assumed to be 425 kg/m^3. The discharge coefficient was considered 0.62 for a sharp-edged leakage hole. Hence, using Eq. (1), the leakage rates at the initial leakage point were calculated accordingly.

Table 4 Leak frequency and leak rate of the LNG bunkering system.

Leak hole size	Frequency (/year)	Leak rate (kg/s)
50 mm [1)]	1.81E-04	19.44
150 mm [2)]	3.16E-06	174.96

Note: [1)] representing all 1-50 mm leak hole cases; [2)] representing all 50-150 mm leak hole cases

3.3 Consequence Analysis

The dispersion model with the geometry of the case ship was designed in the platform of FLACS in consideration of actual bunkering circumstances.

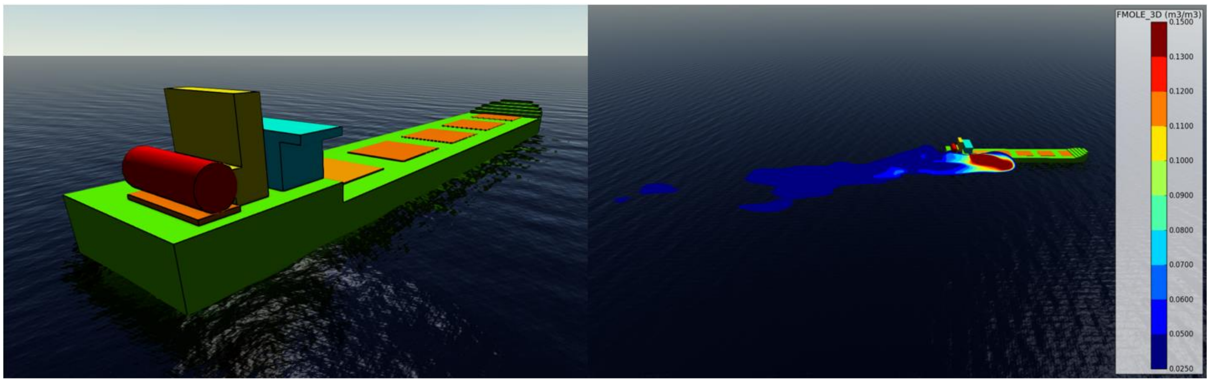

Fig. 7. Geometry and an example result of case ship.

Given the high operational pressure, an LNG release is predisposed to be a jet form. In addition, a part of the leaked liquid is subject to an immediate evaporation as soon as exposed to the ambient condition.

This rapid phrasal transition is described as the 'flashing effect' which is largely determined by operating conditions. In order to implement this phenomenon in the simulation, as described in Fig. 8, the concept of the flash utility, as a function of FLACS, is applied to compensate for the limitations of conventional CFD simulation.

In the meantime, the flash utility is used to identify the point X_f where the initial LNG leak is completely vaporized. In CFD simulation, therefore, we directly used X_f as the point of initiating the dispersion of the air-gas mixture; it should be noted that the volume of the gas mixture at X_f is much more extensive compared to the initially leaked LNG.

Meanwhile, the mixture ratio between the gas and the air at X_f can be determined by means of Eq. (2). According to this, the equivalence mixture ratio was assigned to be 6.7.

$$\text{Equivalence Ratio} = \frac{(\text{mass}_{\text{fuel}}/\text{mass}_{\text{oxygen}})}{(\text{mass}_{\text{fuel}}/\text{mass}_{\text{oxygen}})_{\text{stoichiometric}}} \quad (2)$$

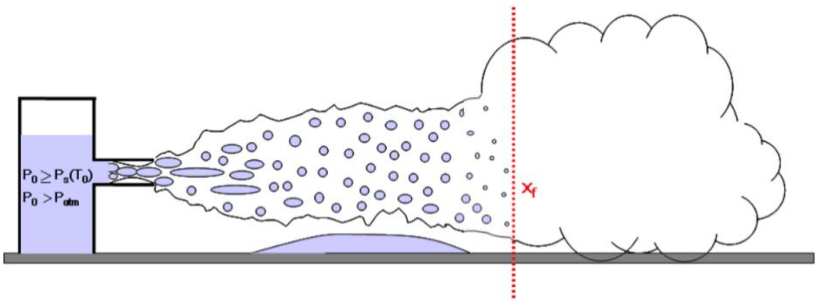

Fig. 8. Flash description in a liquefied gas leakage accident (Gexcon, 2017).

Table 5 Results of flow rate calculations at the entrained point using the flash utility.

Leak Hole Diameter [mm]	**Ambient Temperature [℃]**	**X_f [m]**	**Equivalence Ratio at X_f**	**Jet Leak Area at X_f [m^2]**	**Flow Rate at X_f [kg/s]**
50	20	6.92	6.7	1.64	69.49
150		20.75		14.77	625.42

The critical distances and areas for the 48 scenarios were estimated with the CFD simulation. Given that the effect of gas dispersion was time-dependent, the critical distances were determined at the times when the gas dispersions was observed the widest.

3.4 Risk Assessment

Table 6 Summary of risk assessment results

Scenario analysis	Frequency analysis							Consequence analysis (half-LFL)			Consequence analysis (full-LFL)		
Scenario no.	Leak Hole Diameter	Leak frequency	Leak direction		Wind		Frequency	PDA Max. distance (m)	PIDA Casualties (persons)	Dispersion plot	PDA Max. distance (m)	PIDA Casualties (persons)	Dispersion plot
1	50mm	1.81E-04	Front	0.17	North	0.251	7.56E-06	35.1	5	Fig. 9 (a)	32.1	50	Fig. 10 (a)
2					East	0.197	5.94E-06	24.7	5		27.4	5	
3					South	0.262	7.89E-06	69.6	10		46.6	5	
4					West	0.288	8.68E-06	71.0	10		41.6	5	
5			Back	0.17	North	0.251	7.56E-06	32.7	5	Fig. 9 (b)	28.8	5	Fig. 10 (b)
6					East	0.197	5.94E-06	49.8	5		42.5	5	
7					South	0.262	7.89E-06	45.7	5		31.1	5	
8					West	0.288	8.68E-06	24.0	5		23.4	5	
9			Left	0.17	North	0.251	7.56E-06	24.2	5	Fig. 9 (c)	23.5	5	Fig. 10 (c)
10					East	0.197	5.94E-06	28.0	5		26.9	5	
11					South	0.262	7.89E-06	37.3	5		32.9	5	
12					West	0.288	8.68E-06	80.4	10		37.5	5	
13			Right	0.17	North	0.251	7.56E-06	31.1	5	Fig. 9 (d)	29.4	5	Fig. 10 (d)
14					East	0.197	5.94E-06	71.6	10		40.3	5	
15					South	0.262	7.89E-06	19.2	5		19.2	5	
16					West	0.288	8.68E-06	63.7	10		42.2	5	
17			Top	0.17	North	0.251	7.56E-06	34.9	5	Fig. 9 (e)	16.0	5	Fig. 10 (e)
18					East	0.197	5.94E-06	53.7	10		28.4	5	
19					South	0.262	7.89E-06	45.1	5		35.0	5	
20					West	0.288	8.68E-06	50.3	10		32.1	5	
21			Bottom	0.17	North	0.251	7.56E-06	Less than 10 m	3	-	Less than 10 m	3	-
22					East	0.197	5.94E-06	Less than 10 m	3		Less than 10 m	3	
23					South	0.262	7.89E-06	Less than 10 m	3		Less than 10 m	3	
24					West	0.288	8.68E-06	Less than 10 m	3		Less than 10 m	3	
25	150mm	3.16E-06	Front	0.17	North	0.251	1.32E-07	189.0	50	Fig. 11 (a)	122.6	50	Fig. 12 (a)
26					East	0.197	1.04E-07	402.6	500		115.1	50	
27					South	0.262	1.38E-07	252.5	500		106.9	50	
28					West	0.288	1.52E-07	757.6	1000		500.9	1000	
29			Back	0.17	North	0.251	1.32E-07	770.3	1000	Fig. 11 (b)	287.5	500	Fig. 12 (b)
30					East	0.197	1.04E-07	874.6	1000		392.9	500	
31					South	0.262	1.38E-07	663.4	1000		311.3	500	
32					West	0.288	1.52E-07	380.4	500		132.0	50	
33			Left	0.17	North	0.251	1.32E-07	380.4	500	Fig. 11 (c)	80.1	10	Fig. 12 (c)
34					East	0.197	1.04E-07	362.2	500		182.7	50	
35					South	0.262	1.38E-07	453.1	500		79.7	10	
36					West	0.288	1.52E-07	541.8	1000		293.5	500	
37			Right	0.17	North	0.251	1.32E-07	646.0	1000	Fig. 11 (d)	213.3	500	Fig. 12 (d)
38					East	0.197	1.04E-07	759.1	1000		317.7	500	
39					South	0.262	1.38E-07	413.1	500		93.4	10	
40					West	0.288	1.52E-07	647.3	1000		265.0	500	
41			Top	0.17	North	0.251	1.32E-07	297.6	500	Fig. 11 (e)	124.9	50	Fig. 12 (e)
42					East	0.197	1.04E-07	258.0	500		112.7	50	
43					South	0.262	1.38E-07	321.9	500		126.9	50	
44					West	0.288	1.52E-07	291.5	500		114.5	50	
45			Bottom	0.17	North	0.251	1.32E-07	Less than 10 m	3	-	Less than 10 m	3	-

46					East	0.197	1.04E-07	Less than 10 m	3		Less than 10 m	3	
47					South	0.262	1.38E-07	Less than 10 m	3		Less than 10 m	3	
48					West	0.288	1.52E-07	Less than 10 m	3		Less than 10 m	3	

Table 6 summarises the results of frequency and consequence analyses for all 48 scenarios. The likelihood of each accidental scenario associated with initial gas dispersion behaviour is represented as the results of frequency analysis. On the other hand, the outcomes of the consequence analysis were expressed as forms of both critical distances (from PIDA) and the number of casualties (from PDA) within the critical areas.

3.4.1 *Results of PIDA*

Fig. 9 to Fig. 12 show the critical distance (represented by the maximum length of gas reaching the flammable level) and the critical area (designated by the gas dispersion area within the flammable level) of each scenario. The analysis results reveal that the extent of critical distances/areas is highly sensitive to the initial leak rate; the higher leak rate, the greater the critical zones. In addition, wind direction was shown to be another key parameter to determine the critical areas.

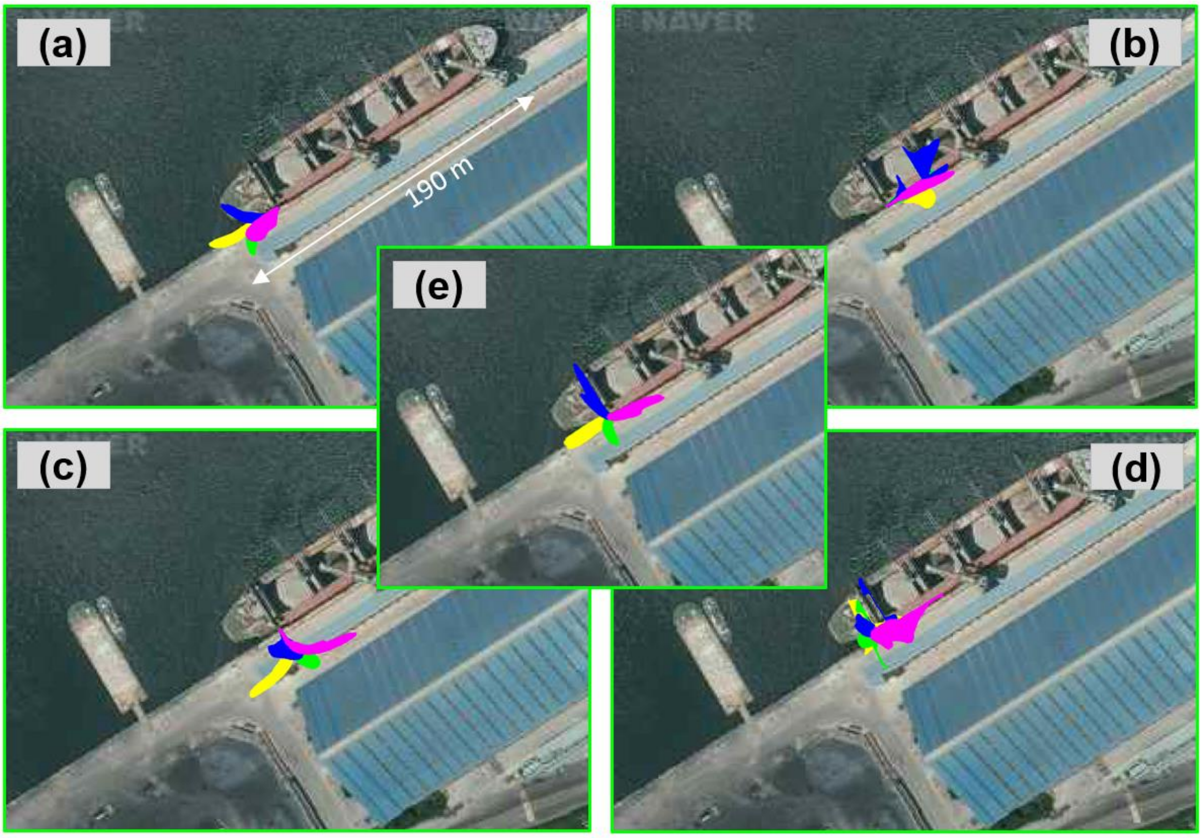

Fig. 9. Gas dispersion plots with half-LFL (2.5% gas concentration in air) for 50 mm leak scenarios (Wind direction: Green-North; Blue-South; Yellow-East; Purple-West).

Fig. 9 shows the results of CFD simulations associated with the 50 mm leak group scenarios: Scenario nos. 1 to 24. The level of critical distance, based on half-LFL criterion, was generally limited to maximum 80.4 m (Scenario no. 12). As shown in Fig. 10, the application of the full-LFL criterion for the same 50 mm leak scenarios narrows the level of critical distances to maximum 46.6 m (Scenario no. 3).

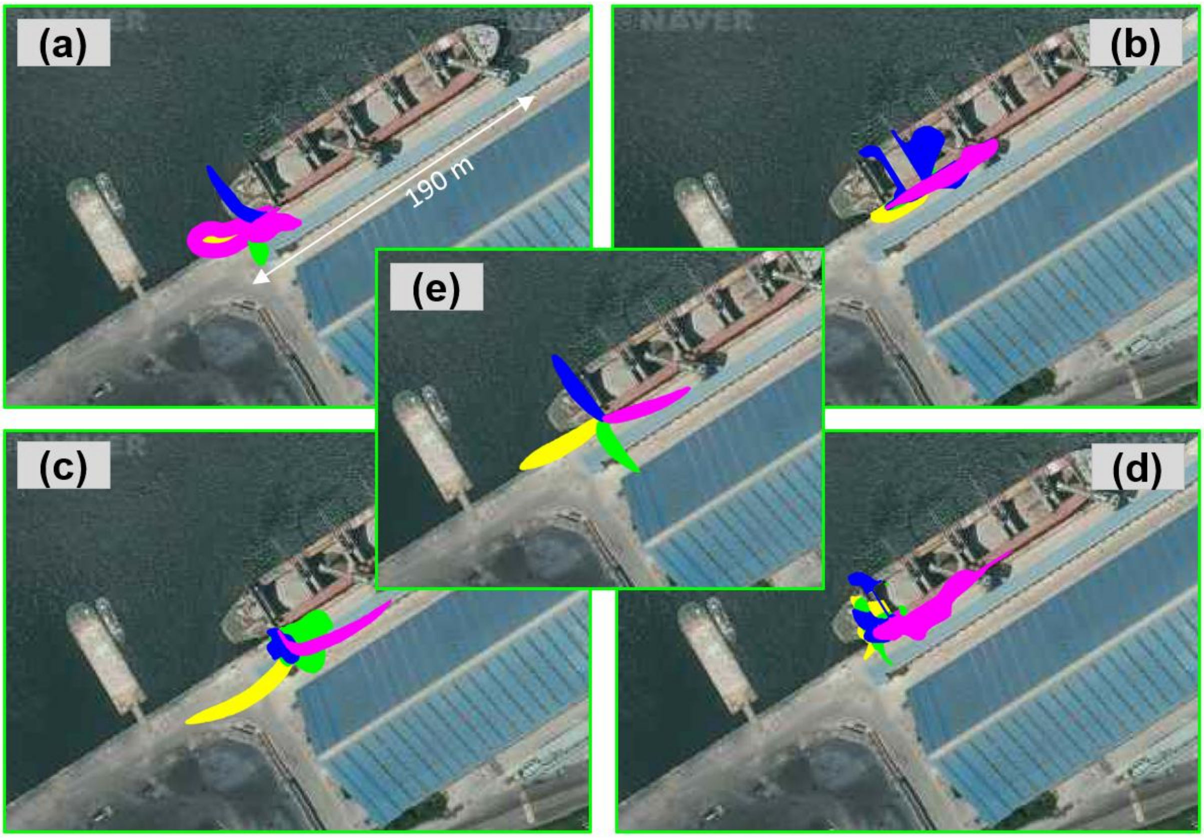

Fig. 10. Gas dispersion plots with full-LEL (5% gas concentration in air) for 50 mm leak scenarios (Wind direction: Green-North; Blue-South; Yellow-East; Purple-West).

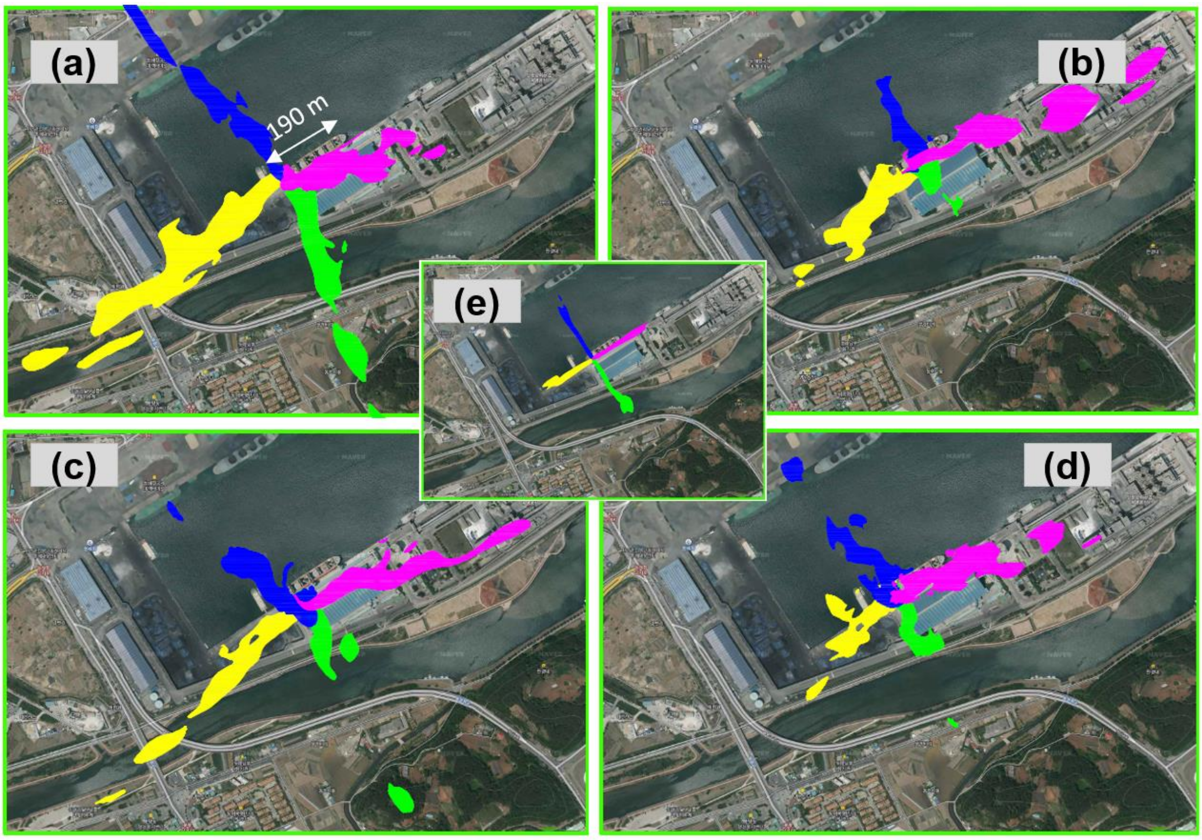

Fig. 11. Gas dispersion plots with half-LFL (2.5% gas concentration in air) for 150 mm leak scenarios (Wind direction: Green-North; Blue-South; Yellow-East; Purple-West).

On the other hand, Fig. 11 illustrates the critical distances and areas for 150 mm leak group scenarios: Scenario nos. 25 to 48 in consideration of half-LFL criterion. The critical distances and areas are revealed much broader compared to the 50 mm leak group scenarios. Maximum 876.4 m was estimated at Scenario no. 30. Using the full-LFL criterion, the results of the same scenarios are plotted in Fig. 12. Slightly moderate, but still wide ranges of critical zones are presented at the maximum.

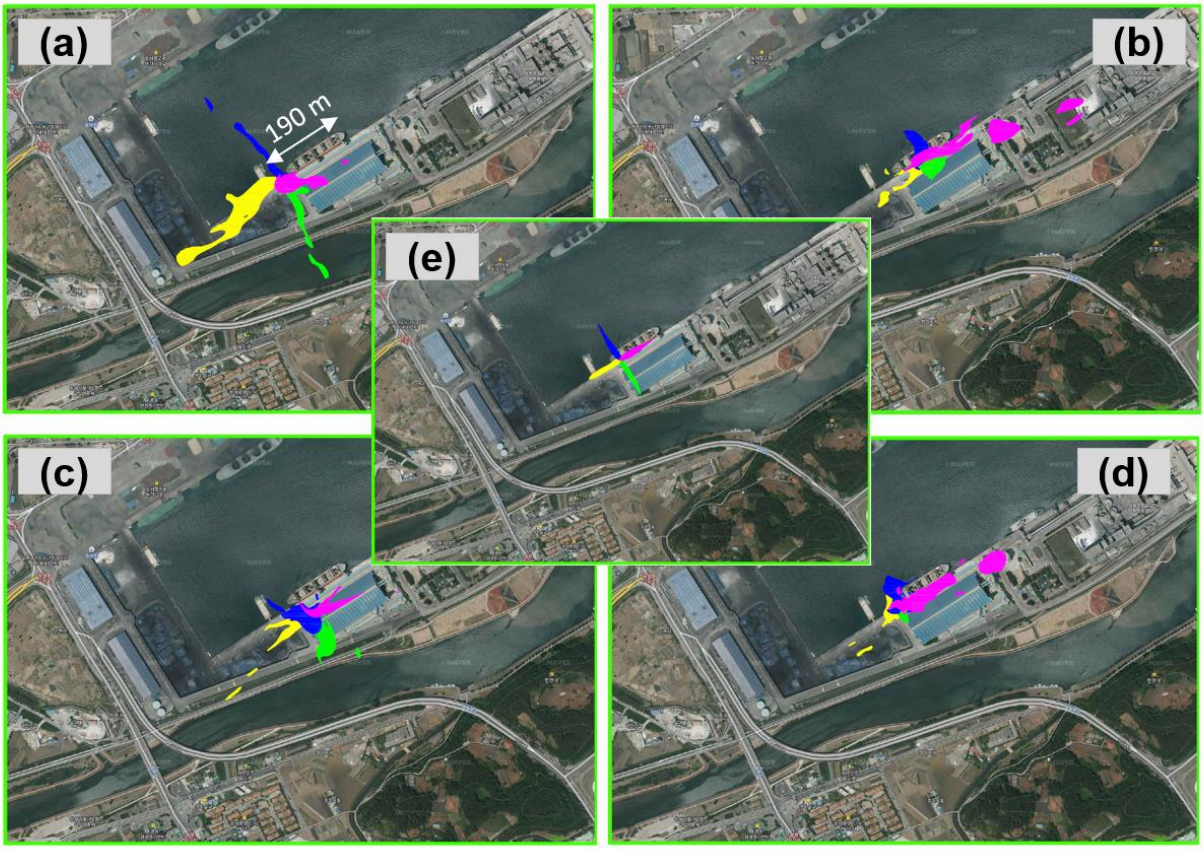

Fig. 12. Gas dispersion plots with full-LEL (5% gas concentration in air) for 150 mm leak scenarios (Wind direction: Green-North; Blue-South; Yellow-East; Purple-West).

In combination between the frequency and the critical area of gas dispersion, the safety zones were established as shown in Fig. 13. Again, it is noteworthy that the risk tolerability will be different, depending on the safety view of port authorities and flag states; although some standards offer some recommendations there is no direct/universal guideline from IMO, thereby port authorities can determine the safety criteria base on their own interest. As a result, some safety evaluators may suggest that one event in every 1,000 year should be acceptable, but some others may ascertain that one event in every 10,000 years would be marginally acceptable. Given this, this paper presents safety zone levels in three different safety criteria: 1E-4 /year, 1E-5/year and 1E-6/year.

Since the safety zones were established based on the boundaries of critical areas, their shapes were not uniform. In order to offer a general insight to port authorities, we regarded the maximum critical distance to be the radius of the safety zone, thereby forming perfect circular shapes in Fig. 14. The results are summarised as below:

- In full-LFL case: 28.8 m in 1E-4 /year criterion, 46.6 m in 1E-5 /year criterion, 213.3 m in 1E-6 /year criterion.

- In half-LFL case: 34.9 m in 1E-4 /year criterion, 80.4 m in 1E-5 /year criterion, 541.8 m in 1E-6 /year criterion.

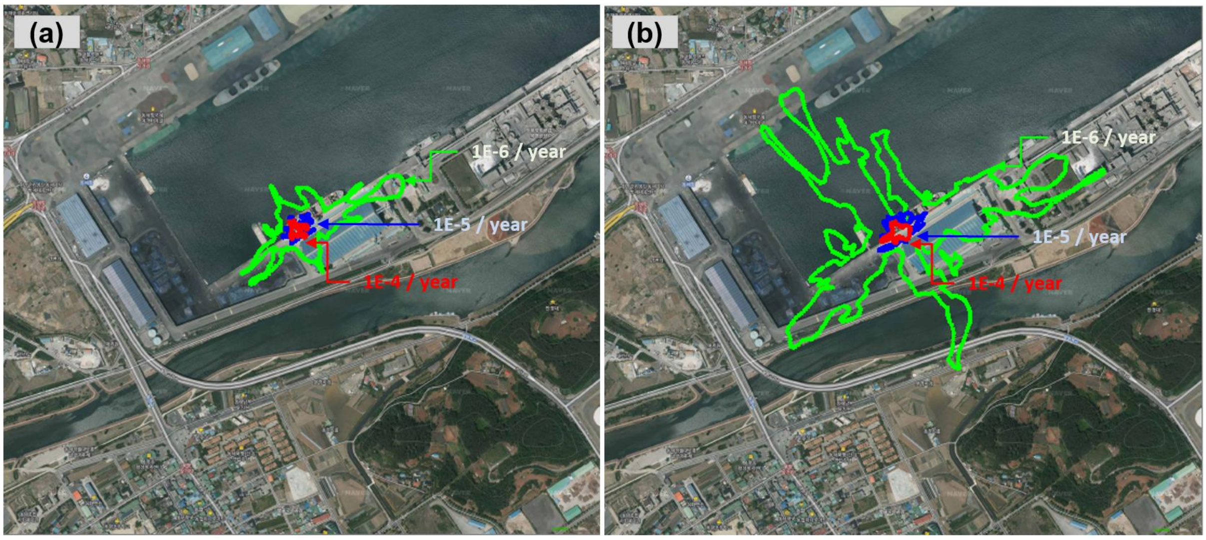

Fig. 13. Safety zones for both (a) full-LFL and (b) half-LFL cases.

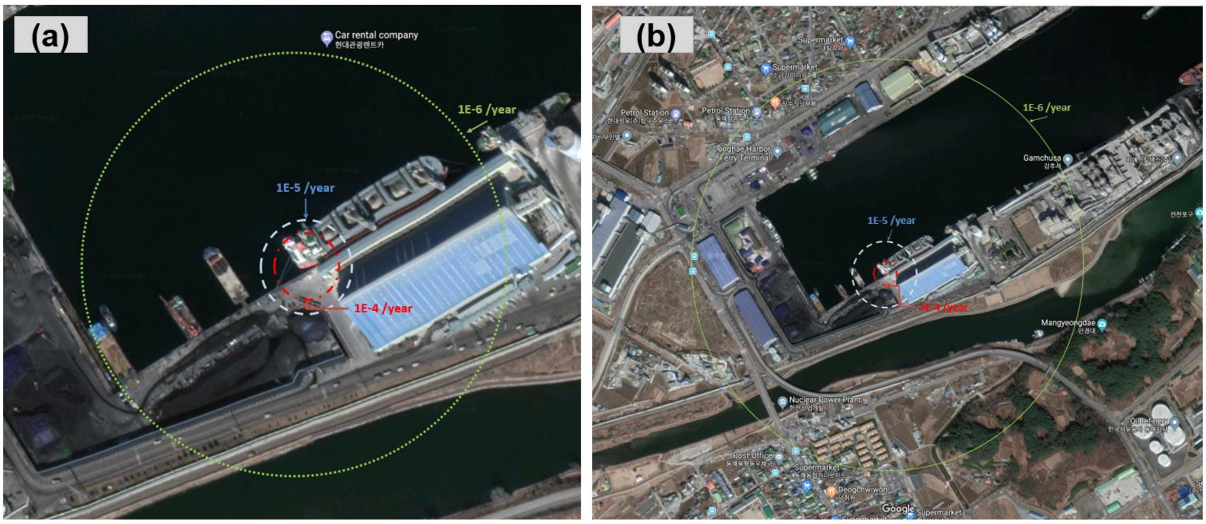

Fig. 14. Safety zones expressed in circle shape for both (a) full-LFL and (b) half-LFL cases.

3.4.2 *Results of PDA*

The results of the PDA were expressed to be the number of casualties, which could help evaluating the proper level of the safety zone pre-established by the PDA. Fig. 15 shows the population-dense area and the number of populations in general; population data was provided by the courtesy of DongHae

Port Authority. With this information, the F-N curve was developed to estimate whether the human risk pertinent to the LNG bunkering for the case ship could be tolerable. As taking a conservative stance, all people within a critical area were considered fatal in this analysis: that is 100% fatality rate. For example, if the critical area was determined in 5 m radius in a scenario and the number of people within this area is five, the number of fatalities were to be considered five.

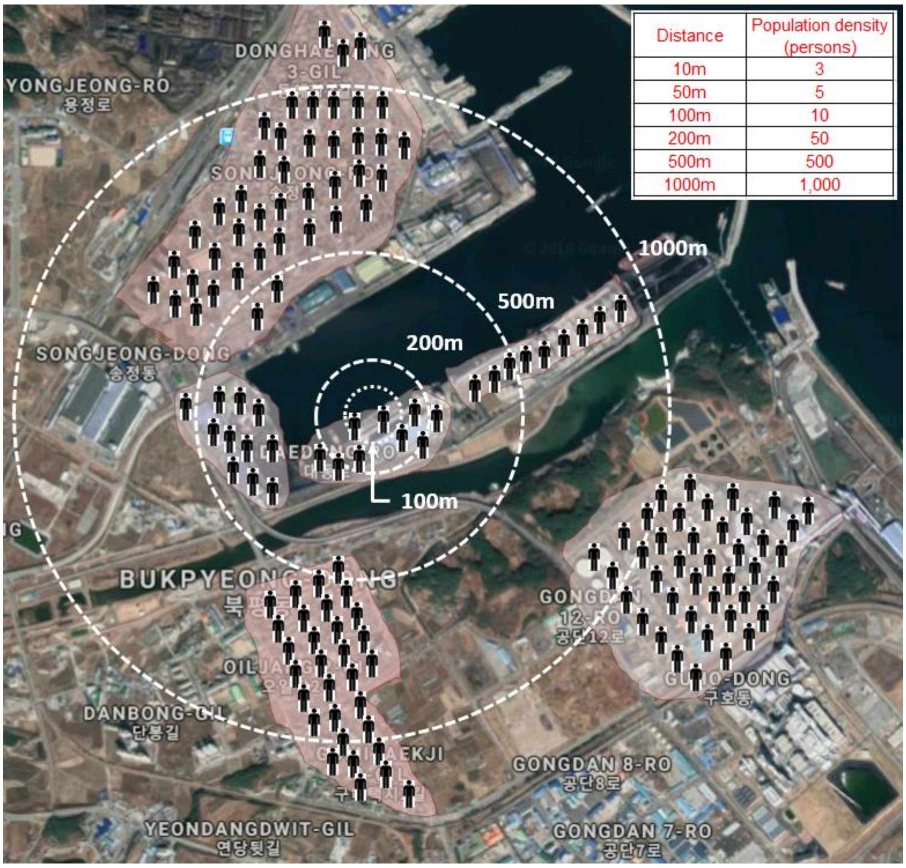

Fig. 15. Population distribution and density at the port.

The association between the probability of occurrence of gas dispersion (thereby flash fire) and the number of fatalities can be presented in an F-N curve that plots the cumulative frequency of gas release that can cause the number of fatalities as described in Table 6. Essentially, the values presented are a measure of how many fatalities per year are implied by the activity of LNG bunkering at Donghae Port.

In Table 6, each scenario of gas dispersion has its own frequency and the number of fatalities. To develop a F-N curve, the outcomes were rearranged from smallest to largest in relation to the number of fatalities (column 1) and an additional column was added for the cumulative frequency that would indicate the frequency of having the number of fatalities or less (column 2).

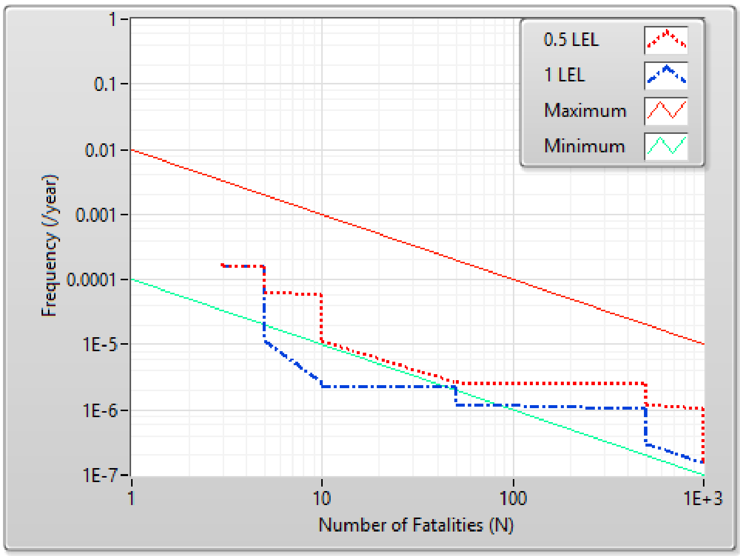

Fig. 16. Relationship between frequency vs the number of fatalities in actual population condition.

By plotting those two columns in a graph, the results of PDA were presented as shown in Fig. 16. The red line describes the maximum tolerable level and the green line indicates the minimum tolerable level; the area below the minimum tolerable level line is regarded 'negligibly small'; the area between the minimum and maximum lines is to be 'tolerable'; the area above the maximum line is 'intolerably high'. Both half-LFL and full-LFL cases are placed within the maximum tolerable level, thereby we can consider this safety level is satisfactory.

Additionally, to investigate the sensitivity of population density on the extent of the safety zones, we have made a series of attempt to deliberately increase the population density. When the population density rose by 20 times a meaningful change in the results were obtained as plotted in Fig. 17 where the status of both half-LFL and full-LFL cases were turned to be 'intolerably high' as parts of their lines exceeded the tolerable level. The lesson of this finding is the importance of considering the human risk using the PDA when establishing a safety zone because the extent of the critical area is more likely to be influenced by the number of people around the area.

Although not directly indicating the proper level of the safety zone, this PDA approach is useful in verifying whether the extent of the safety zone derived from the PIDA is appropriate. Therefore, it will offer pragmatic insights into the establishment of safety zones for LNG bunkering.

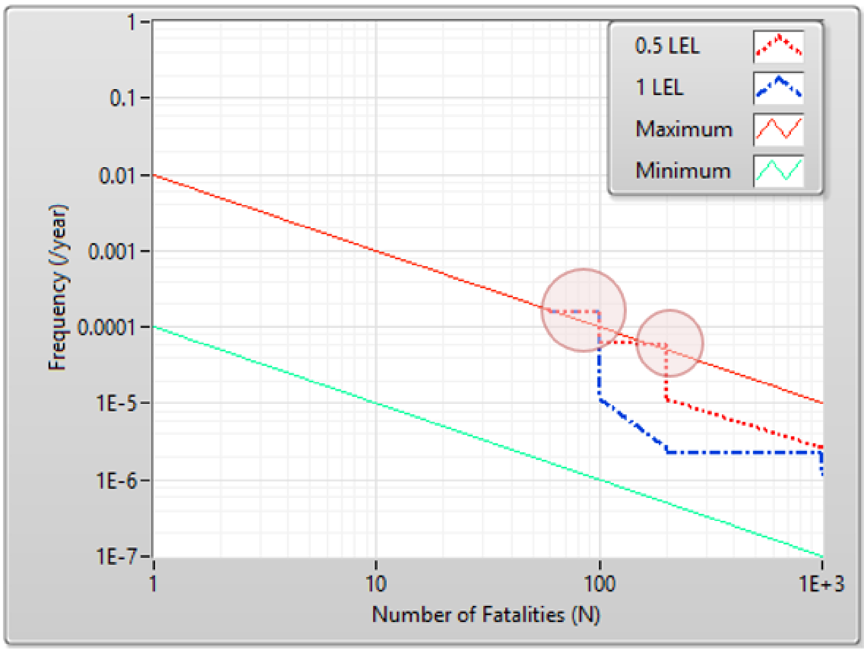

Fig. 17. Relationship between frequency vs the number of fatalities, when the population density is increased by 20 times.

4 Discussion

Although the number of LNG fueled vessels and ports supplying LNG to ships is steadily increasing, a step-by-step guidance on an appropriate approach on how to determine safety zones for LNG bunkering is still deficient. Given that perfect guidelines can only be available after cumulative lessons obtained from multiple studies, we believe the present research is adding some values to keep track on the pathway to achieve this fundamental goal of the marine industry.

The main feature of this paper could be placed on the implementation of the initial idea proposed in the past publication (Jeong et al., 2018), which was limited to introducing the concept of the basic method, but not fully implemented. In this context, this paper is regarded as a continuous research linking past studies and suggests how the proposed method can be applied properly. Therefore, research results could indicate the proper level of the safety zone which can be regarded as realistically applicable to the industry.

While current international codes are not able to provide detailed/comprehensive instructions, the original contribution of this paper can be placed on the fact that approach proposed in this paper offers a structured guidance for performing quantitative risk assessments related to LNG fueled vessels in terms of safe zone determination.

In a way to determine the safety zone, this paper introduced an enhanced approach to transform the 'generally-applicable but less-reliable approach' to 'specifically-applicable and more-reliable one'. In particular, the proposed method conveys significant implications on the importance of considering the PDA as a post-process of the PIDA. Although not directly indicating the proper level of the safety zone, the PDA approach is useful in verifying whether the extent of the safety zone derived from the PIDA is appropriate. It is believed that these research findings will be good inputs for future regulatory frameworks. For example, the case study has shown the effectiveness of the PDA approach against the following fundamental question; *in case that the conventional risk assessment (PIDA alone) guides us to set up a safety zone within 100 meters, we find that there are one or two people in this zone. Do we really need to establish such a huge safety zone for only two people? Conversely, if the decision zone is 10 meters, but the population in this region is more than 20 people. Can we be confident with such a narrow safety zone?*

The purpose of the safety zone is to restrict the unauthorized personals to prevent potential accidents during LNG bunkering. However, according to analysis results, the safety zones may be determined more than 100 m where includes the residential areas. In this situation, it is quite hard to operate the safety zone as it is not practicable to urge residents out of the zones. To remedy this problem, the alternative approach (the double-check with PDA and PIDA) was introduced. The purpose of PDA (using F-N curve) was to confirm the safety level of LNG bunkering even if the residents are still within the zone. In case study, Fig. 16 confirms the safety of LNG bunkering in consideration of the current population. However, if the number of residents are too large (like Fig. 17), we have to re-consider the estimating the safety zone from the beginning or we have to take an action to expel residents out of the zone to ensure the safety level.

In addition, while significant uncertainties associated with massive accidental LNG release during bunkering are present, this research can be regarded to be an active response to international trends of sustainable shipping; in view of the possibly catastrophic consequence of such accidents, the risks associated with LNG bunkering were prudently addressed in this paper. Hence, study results offer us better understanding of the LNG bunkering risk, which will help us to have safer practices and culture of LNG propulsion that arrives in the marine industry. In addition, it is also supportive of enhancing the global competitiveness of marine LNG with healthier, wealthier, safer and more information in proper decision-making.

Another novelty of this paper can be placed on the integration of CFD simulations with the statistical analysis, which is believed the first attempt for the LNG safety analysis. As a result, the outcomes in higher degree of precision and reliability could be obtained throughout the case study. However, as dealing with CFD simulation which claims huge amount of computational time, we had to convince ourselves to focus on the key parameters which may have great influence on the simulation results, whereas the minor parameters were ruled out (the major parameters and minor parameters were determined through a couple of sample simulation as well as based on the knowledge obtained from our past research.). Therefore, it can be said that this present study has a limited scope of analysis to some extent. To enhance the understanding of the correlation between the gas dispersion and environmental conditions, full dynamic analysis should be carried out. In order to understand the correlation of the safety zones with different circumstances, such as various wind speeds, leak hole sizes as well as wind directions, etc., a full dynamic analysis as a future work is essential.

Another limitation of this study can be found in scenario analysis focusing on systematic failure (due to rupture of the bunkering system). Indeed, there are significant chances leading to LNG release other than these system failures. Human error (over 80% of marine accidents are related) can be a good example. Although it is not proper to consider human errors which is largely subjective in various conditions into regulatory works, there still need to develop a guideline to understand the human factors with the extent of the safety zone.

Despite several limitations, this paper is believed to contribute to overcoming the current safety challenges by effectively investigating and presenting a clear guidance of proper risk assessment for establishing LNG bunkering, which can be useful as a general practice as well as for future regulatory framework.

5 Concluding Remarks

1) The shortcomings of existing risk assessments were discussed; their analytical limits brought out uncertainties and possibly misled the conclusions.
2) The effectiveness of enhanced risk assessments has been proven by an integrated approach of PDA and PDIA that can improve the reliability of results by reaffirming the appropriate level of the safety zone.
3) The attempts to combine frequency analysis and CFD simulation results have been shown to be particularly effectual in feasible and enhanced risk assessments.
4) Research findings from the case study with the enhanced model can be highlighted as below:
    - In full-LFL (5 % gas concentration in air), the safety zones were determined to be 28.8 m (in 1E-4 / year criterion), 46.6 m (1E-5 / year criterion) and 213.3 m (1E-6 / year criterion).
    - In half-LFL (2.5 % gas concentration in air), the appropriate levels of the safe zone for the vessel were 34.9 m (1E-4 / year criterion), 80.4 m (1E-5 / year criterion) and 541.8 m (1E-6 / year criterion).

- The safety criteria has a significant influence on the extent of the safety zone. The severe safety criteria was found to contribute to the higher level of safety zones, which gives an insight to port authorities and flag states.
- The proposed model was shown to enhance the safety and reliability of establishing safety zone.

5) The extent of the safety zone proposed in this paper is specific for the case ship. So, it may be possible that different ships and bunkering circumstances will lead to different results as a matter of uncertainty. As a future study, it is necessary to determine the general applicability of the research outputs with dissimilar cases.

Acknowledgement

The authors acknowledge the ILSHIN Marine Transport Co., Ltd. for their valuable support, comments and suggestions. They have contributed significantly to this study particularly for the data collection.

References

ABS, 2012. ABS Guide for Propulsion and Auxiliary Systems for Gas Fuelled Ships.

ABS, 2014. Bunkering of Liquefied Natural Gas-fueled Marine Vessels in North America. ABS, Houston Texas USA.

BV, 2012. Safety Rules for Gas-Fuelled Engine Installations in Ships.

Choi, B.C., Park, K.-H., Doh, D.-H., 2018. Impacts of initial temperature and cylindrical obstacles on the dispersing flammable limits of accidental methane releases in an LNG bunkering terminal. Journal of hazardous materials 355, 104-110.

Corkhill, M., 2018. LNG world Shipping - Healthy freight rates and 2018 LNG shipping predictions.

Dan, S., Lee, C.J., Park, J., Shin, D., Yoon, E.S., 2014. Quantitative risk analysis of fire and explosion on the top-side LNG-liquefaction process of LNG-FPSO. Process Safety and Environmental Protection 92 (5), 430-441.

Dan, S.e.a., 2014. Quantitative risk analysis of fire and explosion on the top-side LNG-liquefaction process of LNG-FPSO. Process Safety and Environmental Protection 92, 430-441.

Dasgotra, A., Teja, G.V., Sharma, A., Mishra, K.B., 2018. CFD modeling of large-scale flammable cloud dispersion using FLACS. Journal of Loss Prevention in the Process Industries 56, 531-536.

DNV, 2011. Part 6 Chapter 13, Gas Fuelled Ship Installations. DNV, Oslo.

DNV, 2012. failure frequency guidance: Process Equipment Leak Frequency Data for use in QRA, Oslo Norway.

DNVGL, 2014. Recommended practice – DNVGL-RP-0006:2014-01: Development and operation of liquefied natural gas bunkering facilities. DNVGL, Oslo.

Gavelli, F., Chernovsky, M.K., Bullister, E., Kytomaa, H.K., 2010. Modeling of LNG spills into trenches. J Journal of hazardous materials 180 (1-3), 332-339.

Gexcon, 2017 FLACS version10.5 user'smanual. Bergen: GexconAS.

Giannissi, S., Venetsanos, A., Markatos, N., Bartzis, J., 2013. Numerical simulation of LNG dispersion under two-phase release conditions. J Journal of loss prevention in the process industries 26 (1), 245-254.

GIE, 2018. The benefits and role of LNG in Europe Providing Europe's Energy Today and in the Future. Gas Infrastructure Europe.

Gopalaswami, N., Kakosimos, K., Zhang, B., Liu, Y., Mentzer, R., Mannan, M.S., 2017. Experimental and numerical study of liquefied natural gas (LNG) pool spreading and vaporization on water. J Journal of hazardous materials 334, 244-255.

Hamutuk, L.o., 2008. Appendix 4. History of accidents in the LNG industry.

Hansen, O.R., Gavelli, F., Ichard, M., Davis, S.G., 2010. Validation of FLACS against experimental data sets from the model evaluation database for LNG vapor dispersion. Journal of Loss Prevention in the Process Industries 23 (6), 857-877.

Iannaccone, T., Landucci, G., Scarponi, G.E., Bonvicini, S., Cozzani, V., 2019. Inherent safety assessment of alternative technologies for LNG ships bunkering. J Ocean Engineering 185, 100-114.

IMO, 2002. MSC/Circ.1023, MEPC/Circ.392: Guidelines for Formal Safety Assessment (FSA) for Use in the IMO Rule-making Process, in: IMO (Ed.), London, UK.

IMO, 2018. RESOLUTION MEPC.304(72) - INITIAL IMO STRATEGY ON REDUCTION OF GHG EMISSIONS FROM SHIPS

ISO, 2013a. 16903: Characteristics of LNG influencing design and material selection, Geneva Switzerland.

ISO, 2013b. ISO 16903: Characteristics of LNG influencing design and material selection.

ISO, 2015a. Guidelines for systems and installations for supply of LNG as fuel to ships. ISO, Geneva Switzerland.

ISO, 2015b. ISO/TS 16901: Guidance on performing risk assessment in the design of onshore LNG installations including the ship/shore interface.

Jeong, B., Lee, B.S., Zhou, P., 2017a. Quantitative risk assessment of fuel preparation room having high-pressure fuel gas supply system for LNG fuelled ship. Ocean engineering.

Jeong, B., Lee, B.S., Zhou, P., Ha, S.-m., 2017b. Evaluation of safety exclusion zone for LNG bunkering station on LNG-fuelled ships. Journal of Marine Engineering & Technology, 1-24.

Jeong, B., Lee, B.S., Zhou, P., Ha, S.-m., 2018. Determination of safety exclusion zone for LNG bunkering at fuel-supplying point. Ocean engineering 152, 113-129.

K, L., 2015. LNG (NG) fuelled shipping – experience and regulations. Norwegian Maritime Authority, Haugesund, Norway.

Lee, S., Seo, S., Chang, D., 2015. Fire risk comparison of fuel gas supply systems for LNG fuelled ships. Journal of Natural Gas Science and Engineering 27, 1788-1795.

Luo, T., Yu, C., Liu, R., Li, M., Zhang, J., Qu, S., 2018. Numerical simulation of LNG release and dispersion using a multiphase CFD model. Journal of Loss Prevention in the Process Industries 56, 316-327.

Norway, G.a., 2012. HAZID report, London.

Parihar, A., Vergara, C., Clutter, J.K., 2011. Methodology for consequence analysis of LNG releases at deepwater port facilities. J Safety science 49 (5), 686-694.

Park, S., Jeong, B., Lee, B.S., Oterkus, S., Zhou, P., 2017. Potential risk of vapour cloud explosion in FLNG liquefaction modules. Ocean engineering.

Park, S., Jeong, B., Yoon, J.Y., Paik, J.K., 2018. A study on factors affecting the safety zone in ship-to-ship LNG bunkering. Ships and Offshore Structures, 1-10.

Pitblado, R., Baik, J., Raghunathan, V., 2006. LNG decision making approaches compared. J Journal of hazardous materials 130 (1-2), 148-154.

Register, L.s., 2011. Rules and Regulations for the Classification of Natural Gas Fuelled Ships. LR, Lloyd's Register.

Sun, B., Guo, K., Pareek, V.K., 2017. Hazardous consequence dynamic simulation of LNG spill on water for ship-to-ship bunkering. J Process Safety Environmental Protection 107, 402-413.

Swuste, P., Groeneweg, J., Van Gulijk, C., Zwaard, W., Lemkowitz, S., 2018. Safety management systems from Three Mile Island to Piper Alpha, a review in English and Dutch literature for the period 1979 to 1988. J Safety science 107, 224-244.

Tan, Z., Li, J., Hu, G., 2014. Risk assessment and countermeasures of gas accidents in the sensitive areas under control during the Olympic Games in Beijing. J Safety science 62, 187-204.

Vílchez, J.A., Villafañe, D., Casal, J., 2013. A dispersion safety factor for LNG vapor clouds. J Journal of hazardous materials 246, 181-188.

Villa, V., Paltrinieri, N., Khan, F., Cozzani, V., 2016. Towards dynamic risk analysis: A review of the risk assessment approach and its limitations in the chemical process industry. J Safety science 89, 77-93.

Wang, H., Oguz, E., Jeong, B., Zhou, P., 2019. Life cycle and economic assessment of a solar panel array applied to a short route ferry. Journal of Cleaner Production 219, 471-484.

Windfinder, 2018. Wind, Wasves & weather forecast.

Woodward, J.L., Pitbaldo, R., 2010. LNG Risk Based Safety: modeling and consequence analysis. John Wiley & Sons.

Appendix

Appendix presenting the results of grid conversion test for the CFD simluation. As shown in the table three different grid sizes were applied for the test: applied grid, coarse grid and fine grid. The simluation conditions were: 150 mm for leak hole diameter, back side of leak direction, East-wind direction at 7 m/s. The test results reveal that the applied model using 2,249,760 meshes does not lead to a significant difference when compared to using the finer grid with 9,919,350 meshes; the deviation was revealed less than 5 %. The coarse grid, on the other hand, had high deviations, thereby being rejected from the simulation.

Table A 1 Information of grid test for the CFD simulation.

<table>
<tr><th>Case</th><th></th><th>X [m]</th><th>Y [m]</th><th>Z [m]</th><th>Results</th></tr>
<tr><td rowspan="3">1. Applied grid</td><td>Min.</td><td>0.5</td><td>0.6</td><td>0.6</td><td rowspan="3">Max. distance [m]
874.6 m</td></tr>
<tr><td>Max.</td><td>40</td><td>40</td><td>20</td></tr>
<tr><td>No. of Grid</td><td colspan="3">2,249,760</td></tr>
<tr><td rowspan="3">2. Coarse grid</td><td>Min.</td><td>1</td><td>1.2</td><td>1.3</td><td rowspan="3">Max. distance [m]
662.6 m</td></tr>
<tr><td>Max.</td><td>60</td><td>60</td><td>30</td></tr>
<tr><td>No. of Grid</td><td colspan="3">442,000</td></tr>
<tr><td rowspan="3">3. Fine Grid</td><td>Min.</td><td>0.3</td><td>0.4</td><td>0.4</td><td rowspan="3">Max. distance [m]
837.4 m</td></tr>
<tr><td>Max.</td><td>20</td><td>20</td><td>10</td></tr>
<tr><td>No. of Grid</td><td colspan="3">9,919,350</td></tr>
</table>

Fig. A 1 Results of grid test (green-coarse grid, Yellow-applied grid, Blue-fine grid).

In addition to Section 2.4, the basic settings and input values of the gas dispersion simulation were further discussed.

Table A 2 leak model.

Property	Value
Type	Jet
Position	Surface on the fuel tank
Size	Depends on the analysis cases (Area was calculated using FLASH utility)
Strat time	10s after analysis (Considering wind build-up time)
Duration	90s
Leak Profile	Parabolic
Leak Shape	Elliptic

FLACS defines leaks as six types: diffusion, mixing, spraying, air, suction and fan. Since the fuel system is pressurized, in the event of a failure, gas leaks would quickly accelerate from inside the system to outside. Hence, the Jet leak type was applied for the simluation. In consideration of the evaporation of

LNG, the jet leakage area was applied to the transferred area calculated using the FLASH utility in FLACS as shown in See Fig. 8.

Table A 3 wind model.

Property	Value
Ambient pressure	100000Pa
Wind speed	7.0m/s
Reference height	10.0m
Wind build-up time	10.0s
Temperature	20℃
Pasquill class*	F (Stable)
Ground roughness	0.0002m
Boundary condition	Wind (Outflow) Nozzle (Inflow)

The wind speed was set at 7 m/s, taking into account the average wind speed of the area being modeled. Ground roughness represents the roughness length for wind profile where 0.0002 m was recommended for the sea surface. While turbulence effect was not considered, non-wind boundaries was recommended as 'Nozzle' by FLACS manual.

Table A 4 Simulation and output control

Property	Value
Analysis time	110s
CFLC*	10
CFLV**	1

***CFLC:** This is a Courant-Friedrich-Levy number based on sound velocity. The value of CFLC connects simulation time step length to control volume dimension through signal propagation velocity.
****CFLV:** This is a Courant-Friedrich-Levy number based on fluid flow velocity. The value of CFLV connects simulation time step length to control volume dimension through signal propagation velocity.

CFLC and CFLV values used for the case studies were more conservative than general CFD analysis cases; CFLC value of 20 and CFLV value of 2 are generally recommended. In this case, it takes more time for simluation but can reduce errors in the results.